

Event-Based Structured Light for Depth Reconstruction using Frequency Tagged Light Patterns

T. Leroux, S.-H. Ieng and R. Benosman

University of Pittsburgh, Carnegie Mellon University, Sorbonne Universit as
benosman@pitt.edu

Abstract—This paper presents a new method for 3D depth estimation using the output of an asynchronous time driven image sensor. In association with a high speed Digital Light Processing projection system, our method achieves real-time reconstruction of 3D points cloud, up to several hundreds of hertz. Unlike state of the art methodology, we introduce a method that relies on the use of frequency tagged light pattern that make use of the high temporal resolution of event based sensors. This approach eases matching as each pattern unique frequency allow for any easy matching between displayed patterns and the event based sensor. Results are show on real scenes.

Index Terms—Neuromorphic sensing, Event-based vision, Structured light, 3D imaging

I. INTRODUCTION

A. Motivation

STRUCTURED LIGHT is considered the most reliable technique to estimate depth and is behind most commonly used methods in the field of non-contact 3D measurement. Because of its accuracy and simplicity, its the method of choice in many applications including autonomous vehicle navigation[1], [2], factory inspection processes [3], [4], object recognition[5], [6] or reverse engineering [7]. The term *structured light* itself refers to the projection of simple or encoded light patterns onto the illuminated scene [8]. Its main purpose is to simplify the extraction of features in the image of the scene captured by a camera, and facilitate the pairing process. Like in classic stereoscopic systems, the measure of 3D information using structured light is done by triangulation when corresponding points are identified.

This paper presents a method based on a completely new neuromorphic vision sensor, whose dynamic and temporal properties are unmatched. Using a totally different approach of vision, it allows to push back the limitations of former systems. Uses of structured light technology can be tracked back to the early 80's [9], but its only since the developement of the Kinect sensor by Microsoft in 2008 that structured light became affordable. A large number of devices have emerged since. However, most of them share two major limitations resulting from the use of classic frame-grabbing cameras. Because they have short dynamic ranges, captured intensity of the projected signal can be extremely low in strong ambient illumination, thus resulting in poor depth estimations. This is especially true in outdoor environnement where sunlight is often 2-5 orders of

magnitude brighter than the projected light. Another constraint is the frequency at which classic cameras operate (between 30 and 120Hz for commonly used cameras), which is not suited to follow and reconstruct fast moving objects. Some of the latest methods using high speed frame-grabbing cameras achieve 3D reconstruction up to 500Hz but at high energy and data cost.

Recent developement in neuromorphic vision opens up new alternatives to classic frame-grabbing cameras and a new way to process visual information. The presented system uses an biomimetic artificial retina with a 143dB dynamic range able to acquire asynchronous data at a microsecond precision.

B. State of the Art

Structured light techniques differs from one another essentially because of the encoding method used to create the projected pattern, or sequence of patterns. In the litterature, several comparative studies can be found that analyse pattern encoding strategies over the last decades [10], [11], [12]. Methods based on multiple patterns (i.e time multiplexing) are generally better when dealing with static objects and offers highly accurate measurements. Posdamer et al. [13] used a succession of patterns generating a pure binary code, followed by works to decrease errors at brightness boundaries [14], increase the resolution [15] or reduce the number of frame needed [16]. For these methods, a high resolution is obtained as depth information is calculated at every pixel. Noise is mostly generated by the movement of objects between successive patterns of the projection. Other methods based on single pattern projection, using spatial multiplexing, are more robust for a moving object. Those includes works on patterns composed of multiple slits of different sizes [17], [18] or colors [19], [20], patterns using specific shapes or colors organized in pseudorandom arrays [21], [22] or direct coding patterns in which each pixel is associated with a unique codeword by either spatial grading [23] or phase shifting [24], [25]. Recently, work has been done aiming to reach real-time reconstruction. Most of these attempts were made using a high speed frame based camera coupled with a fast DLP projector to allow projection of binary patterns at speeds over 1kHz [26], [27]. These methods use both spatial and time multiplexing to get the best from both worlds and achieve up to 500Hz reconstructions, while the current average reconstruction rate is somewhere between 30-100Hz.

II. HARDWARE

A. Time encoded imaging

Biomimetic event-based cameras are a novel type of vision devices that - like their biological counterparts - are driven by "events" happening within the scene. They are not like conventional vision sensors which, by contrast, are driven by artificially created timing and control signals (e.g. frame clock) which have no relation whatsoever to the source of the visual information [28]. Over the past few years, a variety of these event-based devices have been implemented, including temporal contrast vision sensors that are sensitive to relative luminance change [29], [30], gradient-based sensors sensitive to static edges [31], edge-orientation sensitive devices and optical-flow sensors [32]. Most of these vision sensors output visual information about the scene in the form of asynchronous address events (AER) [33] and encode the visual information in the time dimension and not as voltage, charge or current. The presented depth estimation method is designed to work on the data delivered by such a time-encoding sensor.

The ATIS used in this work is a time-domain encoding vision sensors with 304×240 pixels resolution. [28]. The sensor contains an array of fully autonomous pixels that combine an illuminance relative change detector circuit and a conditional exposure measurement block.

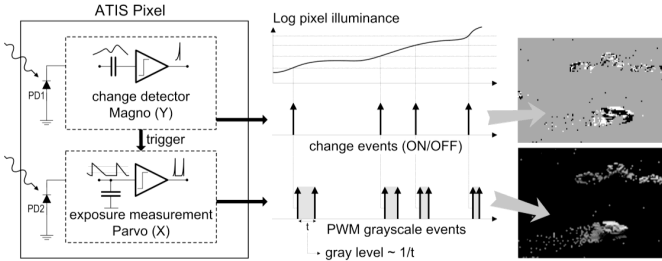


Fig. 1. Functional diagram of an ATIS pixel [29]. Two types of asynchronous events, encoding change and brightness information, are generated and transmitted individually by each pixel in the imaging array.

As shown in the functional diagram of the ATIS pixel in Fig. 1, the relative change detector individually and asynchronously initiates the measurement of an exposure/gray scale value only if - and immediately after - a brightness change of a certain magnitude has been detected in the field-of-view of the respective pixel. The exposure measurement circuit in each pixel individually encodes the absolute instantaneous pixel illuminance into the timing of asynchronous event pulses, represented as inter-event intervals.

Since the ATIS is not clocked like a conventional camera, the timing of events can be conveyed with a very accurate temporal resolution in the order of microseconds. The time-domain encoding of the intensity information automatically optimizes the exposure time separately for each pixel instead of imposing a fixed integration time for the entire array, resulting in an exceptionally high dynamic range and improved signal to noise ratio. The pixel-wise change detector driven operation yields almost ideal temporal redundancy suppression, resulting in a maximally sparse encoding of the image data.

B. Digital Light Processing

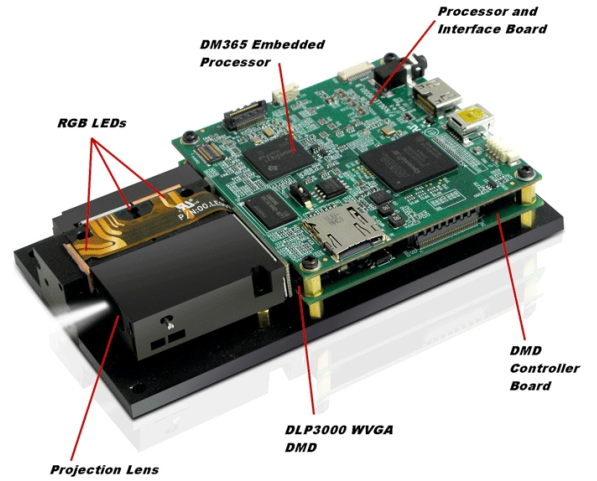


Fig. 2. The DLP lightcrafter module ©

Digital Light Processing (DLP) is an image projection technology originally developed by Texas Instrument, relying heavily on a chip containing orientable micromirrors called Digital Micromirror Device (DMD). A light bulb sends light on the chip's mirror array that reflect light back in a lens to generate an image on the screen. DMD was invented by Hornbeck and Nelson in 1987. In our setup we use a DLP lightcrafter model (Fig. 2) which is a complete projection system embedding a WVGA micromirror array. It is able to project binary frames of 304×240 pixels at a 0.7ms time resolution. Faster and bigger models exist, but this model benefits from the implementation of an asynchronous control driver that enables to manipulate up to 5000 specific mirrors per time step instead of having to modify the complete pixel array synchronously.

C. Setup

For the experiments in this paper we developed an active stereoscopic vision system using the association of an ATIS camera and a DLP projector (Fig. 3). With its very high frame rate, the DMD used to produce binary projection can make profit of the high temporal resolution of the ATIS. An event is conveyed to the output buffer in a few hundred nanoseconds. This means that the time needed to change the position of DMD mirrors is fast enough to obtain spatially and temporally dense information. However limitation arises when exposing the whole pixel array of the ATIS to high frequency changes. An estimation of the maximal event flow the ATIS can currently manage is around 8 mega events per second. Even if this limitation will probably be overcome in the future, a 1kHz stimulation of the sensor is limited to 800 events per step which represents only 1% of the camera's pixel array. Due to this limitation a tradeoff has to be made between temporal and spatial resolution.

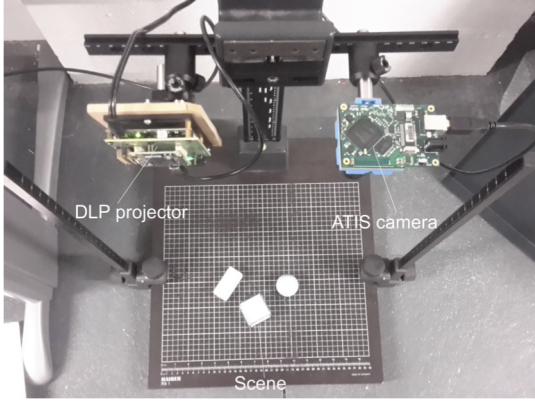


Fig. 3. Experimental setup

III. PATTERN CODIFICATION STRATEGIES

To get the better out of the ATIS sensor, it is mandatory to choose a suitable pattern codification. In the event domain, the only information available is the polarity and timestamp of pixels, thus the correspondance problem can't be solve by color or grey level coding. Moreover, the need for an asynchronous system impose that our pattern can be segmented in small independent patches that we could use to extract local information only when it is needed. This constraint has a direct impact on the spatial organisation of the pattern and direct methods like the one used in ?? must be discarded. In the next section we expand over three different methods that could be used to gather local data independently as well as being decodable without too much computation from the sensor's output to ensure a decent reconstruction speed. The first method we will develop is based on the well known time-multiplexing binary coding (refs?) but encode the binary frames as a signal with set frequency and dutycycle, each element is then part of a spatial codification that can be decoded locally. Our second method aim to make use of spatio-temporal continuity of events generated from fast moving objects to create codewords based on spatial orientation of multiple moving dots. This approach differs only from the first in the way information is extracted from the sensor, but the decoding process is done the same way. Lastly, we developed an approach based on phase-shifting algorithms, but instead of evaluating the phase from several shifted patterns (ref), we continuously move a series of stripes and record precise time difference between stripe positions from an arbitrary origin, which gives us a robust measurement. This last method is able to gather information at the pixel level which is more accurate than previous ones but in exchange the pattern can only be segmented roughly for asynchronous projection.

IV. PERIOD AND DUTYCYCLE

As the ATIS sensor is able to perceive really fast changes in illumination, it is possible to exploit the temporal redudancy of a blinking pattern. This approach can be viewed as an extension of standard binary time-multiplexing methods with the specificity that the different code-words are given by the frequency (and dutycycle) of the signal projected onto a pixel

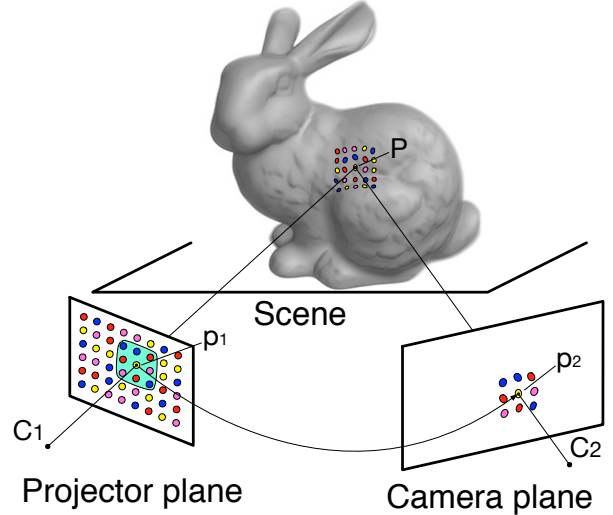


Fig. 4. Structured light principle. A coded light pattern is projected onto the scene that is observed by a camera. Decoding the pattern allows the matching of paired points in the two views (p_1, p_2) and by triangulation of the rays coming from optical centers C_1 and C_2 , the position of the real point P is found. Colors in the picture are for clarity only and in our case refers to different binary signal's dutycycle for the first method or different motion orientation for the second.

instead of being computed through a sequence of intensity values. Fig. ?? shows the pattern spatial organisation, each color refers to a specific dutycycle. It uses a Debruijn sequence that is repeated for each line. Ideally we should have projected full lines instead of small spots but practical limitations limited our choices. A periodic projection generates, at the pixel level, an event stream composed of successive ON and OFF event bursts following the signal's periodic behavior. The length and the number of events constituting each burst is defined by the contrast and illumination condition as well as the set of biases used to operate the sensor.

In a perfect case, each edge of the signal would trigger only one event of the corresponding polarity for each pixel. In this situation, measuring the inter-event time between successive ON and OFF events would be enough to get a correct estimation of the signal's frequency and dutycycle. However, because of small imprecisions in the attribution of timestamps by the sensor's arbiter and possible variations in the global illumination, the number of events triggered at each edge of the signal is not consistent. To ensure at least one event per period, we have two choices: increase the sensor's sensibility to generate bursts at each edge of the signal so that faulty events are less prevalent, or consider a spatial neighborhood instead of a single pixel. The first solution has a major drawback as increasing the number of event at high speed may generate congestion in the event stream and results in less accurate timestamps attribution. The second solution, even if lowering the spatial resolution, is more appropriate.

As a result, instead of considering event streams from each pixel, we create a set of two streams (one for each polarity) composed of events from a local pixel neighborhood of size \mathcal{N} . This operation increase the probability of having at least one

event per edge but also increase the size of bursts. Eventually, using this spatial neighborhood also increase the precision of the timestamp of the first event in each burst as it is always the pixel with the smallest latency that shoot first, reducing the impact of electronic noise in the sensor's chip.

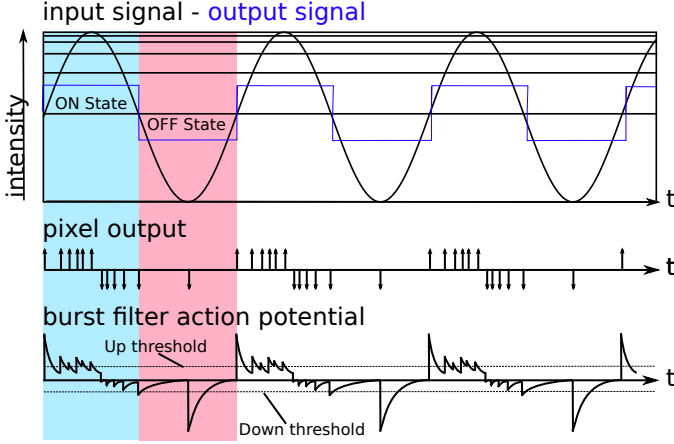


Fig. 5. Example of the burst filter on a sinusoidal input. The input signal is transformed into an event stream by the sensor and at each new event the inter-spike delay is added to the filter's action potential. Between events, the AP follows an exponential decay. At any given polarity state, when the opposite polarity threshold is reached, the output toggles, effectively reflecting the changes of the input signal.

1) *Burst filter*: As we are working on binary pattern, every information related to variations of higher frequency than the signal's one has to be removed. The first step in this process is to reduce the sensor's output, from a series of event clusters following the light variations, to a single event at each edge of the input signal. To recover a robust estimation of the signal period (and duty cycle), it is necessary to clean the bursts and extract, a single, precise event with the correct polarity. A filter is assigned to each pixel's output that integrates inter-event delays as shown on Fig. 5. The filter behaves like two integrate and fire neuron models inhibiting each other but modeled as a single filter, instead of having each neuron triggering when their threshold is reached, it uses a hysteresis function to generate outputs from a single action potential. The filter's action potential is sent through a hysteresis comparator with two different thresholds that enables the control of the sensor dynamics for each polarity. Beginning in an uncertain state at time t_n , when a first threshold $thresh(up, down)$ is reached the output state is changed accordingly and it remains until the opposite polarity threshold is crossed. The variations of the filter's action potential AP then follows the rule: for an event e_i arriving at time t_{n+1} with polarity $p(e_i)$, first the exponential decay is computed as

$$\widehat{AP}(t_n) = AP(t_n) \exp \frac{(t_{n+1} - t_n)}{\tau} \quad (1)$$

with τ a time constant set according to the stimulus frequency, then the update is done by

$$AP(t_{n+1}) = \widehat{AP}(t_n) \cdot (1 + (t_{n+1} - t_n) \cdot p(e_i)), \quad (2)$$

where $p(e_i) = \{-1, 1\}$. Filter's output state $S_{out}(t)$ is modified when the following condition is met:

$$S_{out}(t_{n+1}) = |AP_{n+1}| > thresh(\bar{S}_{out}(t_n)), \quad (3)$$

where $thresh(\bar{S}_{out}(t_n))$ is the absolute value of the opposite polarity threshold for a given output state. Each time this condition is reached, a new event $e(x, y, t, p)$ is triggered and sent to the rest of the filtering chain with (x, y) as the position of the pixel, timestamp t_{n+1} at which the output state changes and the polarity p reflecting filter's new state. The output stream of this filter is a spike train $S_{e(x,y,t,p)}$ with accurate timestamps from which we can easily estimate the signal's frequency $\hat{f}(x, y)$ after each spike of same polarity by

$$\hat{f}(x, y) = \frac{1}{\hat{T}} = \frac{1}{t_k^p - t_{k-1}^p}. \quad (4)$$

The signal's duty cycle is estimated from the computation of its two half periods by comparing the successive alternations of positive and negative filtered events as

$$\hat{T}_k^{ON} = (1 - \lambda)\hat{T}_{k-1}^{ON} + \lambda(t_k^{OFF} - t_{k-1}^{ON}), \quad (5)$$

$$\hat{T}_k^{OFF} = (1 - \lambda)\hat{T}_{k-1}^{OFF} + \lambda(t_k^{ON} - t_{k-1}^{OFF}), \quad (6)$$

with λ a smoothing parameter.

The signal's duty cycle is given by

$$\hat{\alpha} = \frac{\hat{T}_k^{ON}}{\hat{T}_k^{ON} + \hat{T}_k^{OFF}}. \quad (7)$$

Results of the method are shown in Fig. 6 for a wide range of frequencies going from 40Hz and up to 1kHz. Bias settings of the sensor were fixed during the experiment and chosen to cover the complete range of frequencies without changing the behavior of event bursts to reduce the influence of background noise, however the threshold for the OFF channel was a bit too low at 1kHz and no output could be recorded. This doesn't mean that the algorithm can't extract frequencies over 1kHz, but such high speed requires a particular bias setting. The scope of this paper is to present a pattern design for structured light reconstruction and as such, bias settings should be set in order to optimize the behavior in a narrower range of frequencies around the desired projection rate.

Error bars shows the standard deviation over the 100 periods measured at each frequency. Looking at the ON events results for 500Hz and 666Hz, we can see that the consistency of the frequency estimation is heavily dependent on the good quality of the data recorded: at those two frequencies, the number of ON events recorded fell to only one third of those of negative polarity, which translates into missed edges or inaccurate timestamps on the filter's output. The reason of this drop in events number at particular frequencies is yet unknown but could lay in ambient light condition or background noise. The OFF channel offers more consistency and we can observe a slight increase in variance for high frequencies that express the progressive influence of small imprecision in timestamp attribution as the period decrease closer to the sensor's temporal resolution.

In Fig. 7 we show the error in percentage of the projected frequency, obtained for a signal blinking at 1kHz, over 500

periods. We obtain a mean extracted frequency $\hat{f} = 999.92\text{Hz}$ for a 3×3 neighborhood and the error stays under 3%, which corresponds to a standard deviation of $\sigma = 9.19\text{Hz}$.

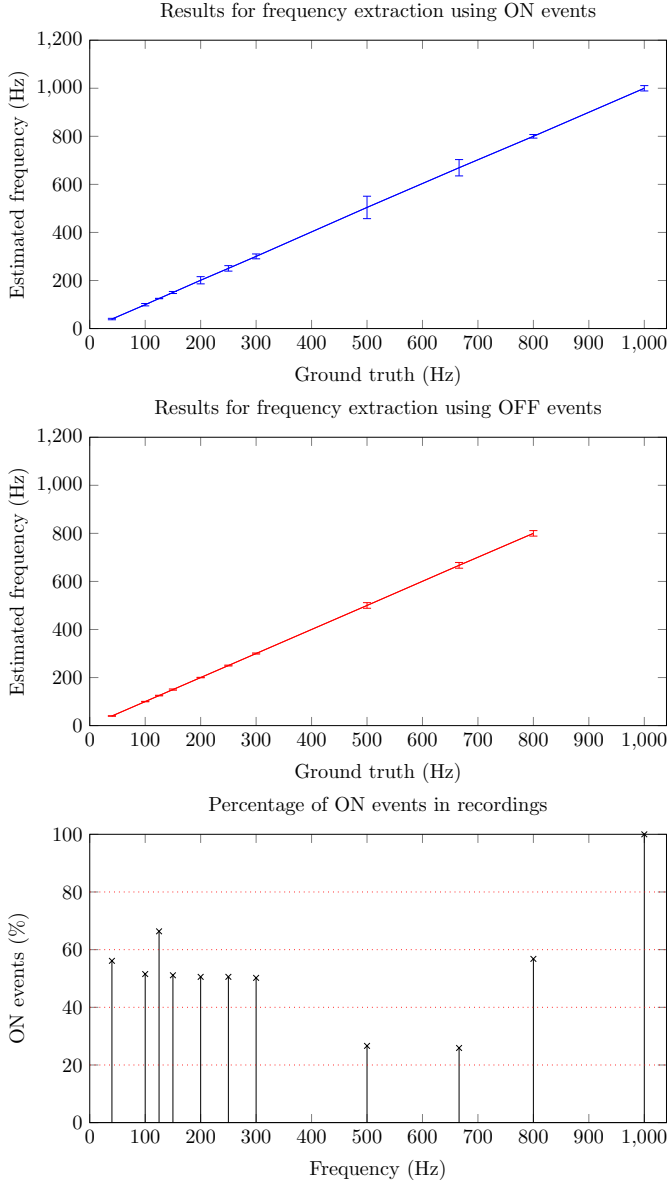


Fig. 6. Results for frequencies ranging from 40Hz to 1kHz over 100 periods. Error bars shows the standard deviation observed in each set. Duty cycle was fixed at 50%. The third graph shows the percentage of ON events in each set and can explain variations of the variance observed at 500Hz and 666Hz.

A. Random shifting

Given a set of n signals following a square wave of fixed frequency, with no other treatment done, every signals switch at the same time and will generate at least $2n$ events (ON and OFF alternance) for each period T if used in projection on the ATIS. What we desire is an asynchronous stimulus. Here, not only it is totally synchronous, but it is also eventually a large number of changes for a single time step. We need to lower this number as much as possible to stay under practical limitations and generate smooth activity on the sensor. To ensure that,

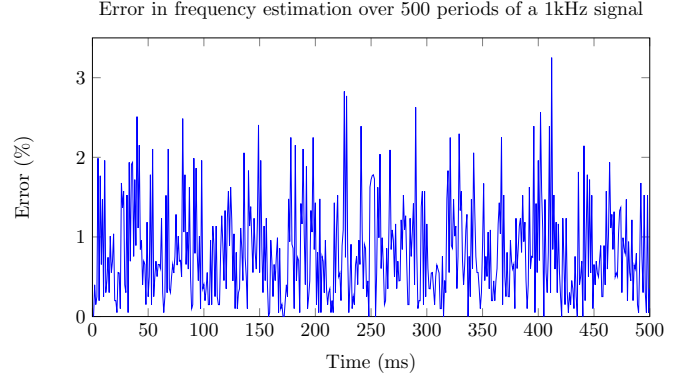


Fig. 7. Error percentage in frequency estimation, for 500 periods of a signal at 1kHz in a 3×3 pixel neighborhood. The algorithm gives an estimation maintained under less than 3% error.

we introduce a random phase shift for every pixels in the set with uniform distribution so that the probability p of having a change event X in a time window of size Δt is

$$\begin{aligned} p(X) &= p(t \leq X \leq t + \Delta t) \\ &= \int_t^{t+\Delta t} \frac{2}{T} d\tau \\ &= \frac{2\Delta t}{T} \end{aligned} \quad (8)$$

The number of changes generated by the whole set of phase shifted pixels follows a binomial distribution $\mathcal{B}(n, p)$ with average value $\mu = np$ and variance $\sigma^2 = np(1 - p)$ as shown in Fig.??.

In a coded pattern constructed from an alphabet of size k , we have k sets of pixel with same frequency so the distribution of the total number of changes would be the sum of each binomial functions $\mathcal{B}_k(n_k, p_k)$. An approximation of this sum can be found by a normal distribution $\mathcal{N}(\mu, \sigma)$ as long as σ^2 is not too small with

$$\mu = \sum n_k p_k \quad \sigma^2 = \sum n_k p_k (1 - p_k) \quad (9)$$

V. ORIENTATION TRACKING

This second method aims to take advantage of the powerful tracking capabilities of the ATIS sensor as it has been demonstrated in ???. Instead of using only time to code the symbols of the pattern, a spatio-temporal code is designed. Spots are moved along different oriented axis in a pattern organized in the same way than the previous method. Tracking is done using gaussian kernels designed in the previously cited paper and, for each determined position, orientation of the moving axis is computed from the covariance matrix by determining the highest correlation axis. Compared to the first method's codification, tracking enables to gather information much faster, as each successive projection step improve the current tracker covariance instead of having to wait a complete period. The acquisition can be made each time the trackers are updated and this delay can be set lower than a complete movement revolution. However, the spatial resolution is lowered by the

size of the moving object and symbol density cannot be too high or the tracking would fail to separate symbols from each other.

A. Perfect Maps

Perfect Maps, are random arrays of dimensions $r \times v$ in which a sub-matrix of dimensions $n \times m$ appears only once in the whole pattern. Theoretically, PM are constructed having dimensions $rv = 2^{mn}$ but usually the zero-matrix is not considered giving $rv = 2^{mn} - 1$ unique sub matrices of $m \times n$ dimensions. In [], Morano defines a brute force algorithm (non De Bruijn based) to generate these maps by adding successive pseudo-random elements to the pattern, row by row starting from the top left corner. Each new element corresponds to a new sub matrix with an associated code with alphabet of size k , and its Hamming distance between all codes already included in the pattern is calculated. If this distance is superior or equal to the minimum Hamming distance specified, the test is passed and the code is added, otherwise the other $k - 1$ symbols are tested. When the algorithm gets stuck, the whole pattern is canceled and the algorithm starts over. Since the constructed pattern can contains only a subset of all possible combinations, such PM is called Perfect SubMaps (PSM). Other works used this brute force approach like Claes [] using a colour codification or Albitar [] with geometrical features. More recently, Maurice and al. [] proposed a hybrid algorithm to build large patterns of more than 200×200 features in a very short time with high Hamming distance, using a splitting strategy to perform the Hamming test in the codeword space instead of the pattern array. We choose to use in this paper an algorithm inspired by this last method.

To generate a matrix M, with a number of symbols k and a codeword length n , we first create an array with k^n boolean flags for all possible codewords, initialised to zero. Starting on the top left corner of M, we randomly generate a first 3×3 patch and perform a Hamming test on every codewords with a distance $H < H_{min}$. Each flag array entry is accessed by a single codeword such that the n symbols are the coefficients in k basis. If all the corresponding flags are set to *false*, the patch is added to M and a next patch is generated until the map is complete (Fig.??). If the algorithm gets stuck in a situation were the added symbol generates only forbidden codes, we shuffle recently added codes until all neighboring codes affected by this modification pass the Hamming test.

VI. PHASE SHIFTING

Phase shifting is a well known method since 1966 (Carr, 1966) that has been widely used in interferometry for its better accuracy and speed as opposed to static images analysis methods. PS algorithms records a series of images that encode the wavefront phase in the variations of the intensity pattern. Various algorithms has been developed over the years using different number of images and phase unwrapping methods. Similarly, fringe projection for 3D shape reconstruction has been exhaustively studied because of its simple setup and processing associated with relatively high speed and resolution and among those, phase-shifting methods have proven very

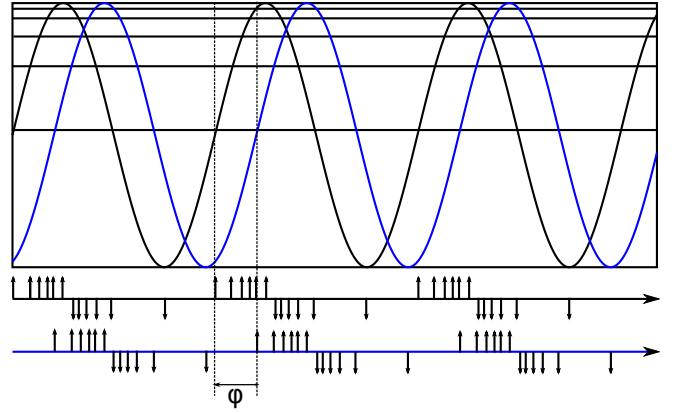


Fig. 8. When a periodic signal is continuously shifted in front of the sensor, the event stream of two different pixels gives precise temporal information about the phase of the signal.

effective. In standard imaging, intensity values of successive shifted patterns are compared point-to-point to recover a unique phase value for each parallel line along the coding axis. The existence of a depth discontinuity in the scene will cause a deformation of the projected pattern that will be recorded as a phase deviation as shown on Fig. ???. The unique phase value recovered is matched with the projected pattern and the shape of the scene objects can be computed.

A. Event-base phase-shifting

Commonly, in order to recover phase deviation, several phase-shifted patterns are projected and recorded. Using a set number of shifted images, a system of equations is defined and solving it allows to retrieve the phase value. With AES sensors however, no intensity value can be measured directly and no complete frames can be acquired which makes common methods unusable. Instead, a continuous shifting of the pattern is used to produce on each line along the coding axis, a series of events with precise timestamps following the variations of the pattern fringes. Every period of the signal projected generates on each pixels a succession of alternatively positive and negative spike bursts $\mathcal{S}(p)$ as shown in Fig. 8. Taking a given pixel p_i as reference on a line, for every pixels $p_j, \forall j \neq i$, we can measure the time-shift between bursts $\mathcal{S}(p_j)$ and $\mathcal{S}(p_i)$. To recover the wrapped phase ϕ , a modulo operator is applied on this value to constrain it between 0 and the signal's period, then it is projected on the interval $[0, 2\pi)$ by :

$$\phi = \frac{2\pi}{P_{signal}} \text{mod}(\Delta t(\mathcal{S}(p_j), \mathcal{S}(p_i)), P_{signal}) \quad (10)$$

An unwrapping algorithm is used to compute the absolute phase value Φ for every pixels. On each line along the coding axis, the following recursive formula is applied :

$$\Phi_x = \Phi_{x-1} + \lambda * \text{mod}(\phi_{x-1} - \Phi_{x-1}, 2\pi) \quad (11)$$

Once the unwrapped phase is obtained, a mapping between the projected pattern and the phase image can be found and the 3D measurement is done.

VII. RESULTS

A. Experiment

The method is applied on a scene containing two objects placed around one meter away from the system. We used a SPSM of 20×30 symbols and the pattern codification is done using the duty cycle of the signal. The neighborhood in the burst filter is set to 1 (3×3 pixels) and signal's frequency is set to 20Hz for performance issues. The algorithm runs on MatLab and even if it could be heavily parallelized, it wasn't the case on this experiment and real time wasn't achieve. An image of accumulated outputs from filters is given in Fig. 9, colors in the image reflect the estimation of the duty cycle by each pixel associated filter. Point correspondance is performed by extracting the 3×3 duty cycle based codewords and as pattern's dots are bigger than a single pixel, we perform a spatial averaging to obtain a sub-pixel position of the dot in the camera frame. After triangulation, a 3D point cloud is obtained (Fig. 10)

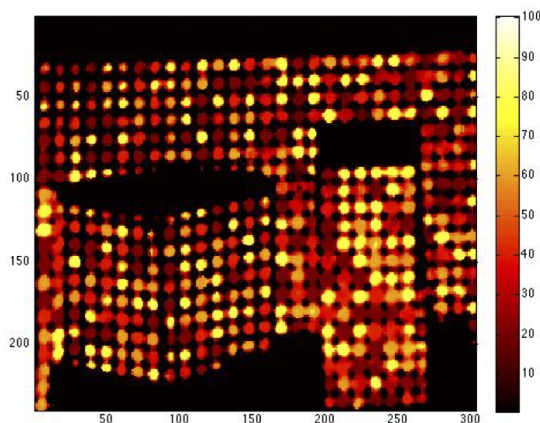


Fig. 9. Image of the projected pattern as extracted by the algorithm. Colors correspond to the estimated duty cycle.

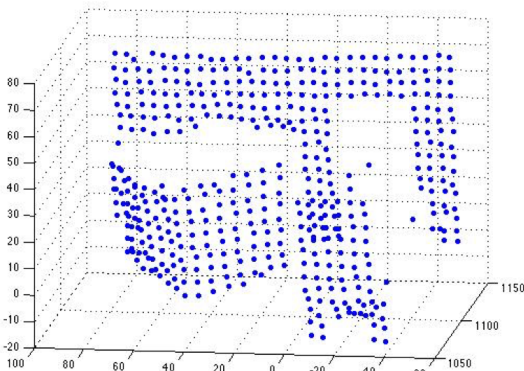


Fig. 10. 3D point cloud.

VIII. CONCLUSION AND DISCUSSION

This paper introduced a methodology that makes use of the high temporal resolution of the event based sensor to rethink the problem of structured light depth reconstruction. We used

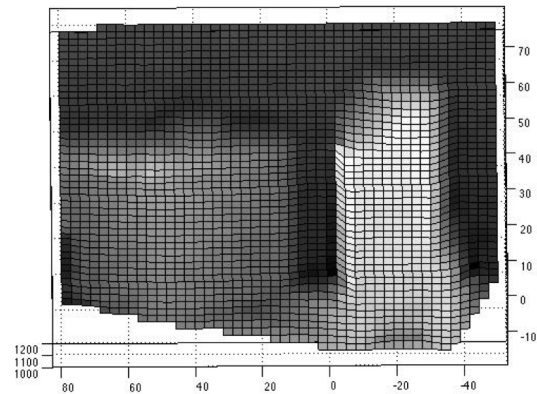


Fig. 11. Reconstructed depth

a unique spatial distribution of light patterns composed of elements each flickering at a unique frequency. We also used the idea of random shift allowing each neighborhood to be unique. Each methodology relying on the combined use of an event based camera and a light projector coding each spatial position in the frequency domain can make use of the developed approach. There are several ways to decode frequencies from the output of the event based camera. The method used here could be bettered, using more precise event based camera allowing frequency to be extracted from the timing of the oscillation of each pattern from inter spike information. If that condition is fulfilled even simpler patterns could be used without the need to rely on unique neighborhoods.

REFERENCES

- [1] A. D. L. Escalera, L. Moreno, M. A. Salichs, and J. M. Armingol, "Continuous mobile robot localization by using structured light and a geometric map," *International Journal of Systems Science*, vol. 27, no. 8, pp. 771–782, 1996. [Online]. Available: <http://www.tandfonline.com/doi/abs/10.1080/00207729608929276>
- [2] M. Asada, "Map building for a mobile robot from sensory data," *Systems, Man and Cybernetics, IEEE Transactions on*, vol. 20, no. 6, pp. 1326–1336, 1990.
- [3] Y. Kakinoki, T. Koezuka, S. Hashinami, and M. Nakashima, "Wide-area, high dynamic range 3-d imager," in *Proc. SPIE 1194, Optics, Illumination, and Image Sensing for Machine Vision IV*, 1990.
- [4] R. T. Chin, "Automated visual inspection: 1981 to 1987," *Computer Vision, Graphics, and Image Processing*, vol. 41, no. 3, pp. 346–381, 1988. [Online]. Available: <http://www.sciencedirect.com/science/article/pii/0734189X88901089>
- [5] E. M. Petriu, Z. Sakr, H. J. W. Spoelder, and A. Moica, "Object recognition using pseudo-random color encoded structured light," in *Instrumentation and Measurement Technology Conference, 2000. IMTC 2000. Proceedings of the 17th IEEE*, vol. 3. IEEE, 2000, pp. 1237–1241. [Online]. Available: http://ieeexplore.ieee.org/xpls/abs_all.jsp?arnumber=848675
- [6] J. Park, G. N. DeSouza, and A. C. Kak, "Dual-beam structured-light scanning for 3-d object modeling," in *3-D Digital Imaging and Modeling, 2001. Proceedings. Third International Conference on*. IEEE, 2001, pp. 65–72. [Online]. Available: http://ieeexplore.ieee.org/xpls/abs_all.jsp?arnumber=924399
- [7] D. Page, A. Koschan, Y. Sun, and M. Abidi, "Laser-based imaging for reverse engineering," *Sensor Review*, vol. 23, no. 3, pp. 223–229, 2003. [Online]. Available: <http://www.emeraldinsight.com/journals.htm?issn=0260-2288&volume=23&issue=3&articleid=876385&articletitle=Laser-based+imaging+for+reverse+engineering&>
- [8] R. Klette, K. Schlüns, and A. Koschan, *Computer vision: three-dimensional data from images*. Springer Singapore, 1998, vol. 20. [Online]. Available:

- http://www.researchgate.net/publication/220689403_Computer_vision_-_three-dimensional_data_from_images/file/32bfe50d203e8594ea.pdf
- [9] J. Batlle, E. Mouaddib, and J. Salvi, "Recent progress in coded structured light as a technique to solve the correspondence problem: a survey," *Pattern recognition*, vol. 31, no. 7, pp. 963–982, 1998. [Online]. Available: <http://www.sciencedirect.com/science/article/pii/S0031320397000745>
 - [10] X. Su and W. Chen, "Fourier transform profilometry: a review," *Optics and Lasers in Engineering*, vol. 35, no. 5, pp. 263–284, may 2001. [Online]. Available: [https://doi.org/10.1016/S0143-8166\(01\)00023-9](https://doi.org/10.1016/S0143-8166(01)00023-9)
 - [11] J. Salvi, J. Pags, and J. Batlle, "Pattern codification strategies in structured light systems," *Pattern Recognition*, vol. 37, no. 4, pp. 827–849, april 2004. [Online]. Available: <http://www.sciencedirect.com/science/article/pii/S0031320303003303>
 - [12] J. Salvi, S. Fernandez, T. Pribanic, and X. Llado, "A state of the art in structured light patterns for surface profilometry," *Pattern Recognition*, vol. 43, no. 8, pp. 2666–2680, aug 2010. [Online]. Available: <http://www.sciencedirect.com/science/article/pii/S003132031000124X>
 - [13] J. L. Posdamer and M. D. Altschuler, "Surface measurement by space-encoded projected beam systems," *Computer graphics and image processing*, vol. 18, no. 1, pp. 1–17, 1982. [Online]. Available: <http://www.sciencedirect.com/science/article/pii/0146664X8290096X>
 - [14] S. Inokuchi, K. Sato, and F. Matsuda, "Range imaging system for 3-d object recognition," in *Proceedings of the International Conference on Pattern Recognition*, vol. 48, 1984, pp. 806–808.
 - [15] D. Bergmann, "New approach for automatic surface reconstruction with coded light," in *SPIE's 1995 International Symposium on Optical Science, Engineering, and Instrumentation*, 1995, pp. 2–9. [Online]. Available: <http://proceedings.spiedigitallibrary.org/proceeding.aspx?articleid=1007846>
 - [16] a. D.Caspi, N.Kiryati, "Range imaging with adaptive color structured light," *IEEE Transactions on Pattern Analysis and Machine Intelligence*, vol. 20, no. 5, pp. 470–480, 1998.
 - [17] M. Maruyama and S. Abe, "Range sensing by projecting multiple slits with random cuts," *IEEE Transactions on Pattern Analysis and Machine Intelligence*, vol. 15, no. 6, pp. 647–651, 1993.
 - [18] J. T. N. Durdle and V.Raso, "An improved structured light technique for surface reconstruction of the human trunk," in *IEEE Canadian Conference on Electrical and Computer Engineering*, IEEE, Ed., vol. 2, 1998, pp. 874–877.
 - [19] L. Zhang, B. Curless, and S. Seitz, "Rapid shape acquisition using color structured light and multi-pass dynamic programming," in *First International Symposium on 3D Data Processing Visualization and Transmission*, 2002, pp. 24–36.
 - [20] J. Salvi, J. Batlle, and E. Mouaddib, "A robust-coded pattern projection for dynamic 3d scene measurement," *Pattern Recognition Letters*, vol. 19, no. 11, pp. 1055–1065, 1998. [Online]. Available: <http://www.sciencedirect.com/science/article/pii/S0167865598000853>
 - [21] P. G. C. Albitar and C. Doignon, "Design of a monochromatic pattern for a robust structured light coding," in *IEEE International Conference on Image Processing*, IEEE, Ed., vol. 6, 2007, pp. 529–532.
 - [22] X. Maurice, P. Graebing, and C. Doignon, "A pattern framework driven by the hamming distance for structured light-based reconstruction with a single image," in *IEEE Conference on Computer Vision and Pattern Recognition*, IEEE, Ed., 2011, pp. 2497–2504.
 - [23] J. Tajima and M. Iwakawa, "3-d data acquisition by rainbow range finder," in *International Conference on Pattern Recognition*, IEEE, Ed., vol. 1, 1990, pp. 309–313.
 - [24] C. Guan, L. Hassebrook, and D. Lau, "Composite structured light pattern for three-dimensional video," *Optics Express*, vol. 11, no. 5, pp. 406–417, 2003. [Online]. Available: <http://www.opticsexpress.org/abstract.cfm?URI=oe-11-5-406>
 - [25] T. K. N. Ono, T. Shimizu and S. Ando, "Real-time 3d image based on spatio-temporal phase unwrapping," in *SICE 2004 Annual Conference*, vol. 3, 2004, pp. 2544–2547.
 - [26] K. D. I. Ishii, K. Yamamoto and T. Tsuji, "High-speed 3d image acquisition using coded structured light projection," in *International Conference on Intelligent Robots and Systems*, IEEE, Ed., 2007, pp. 925–930.
 - [27] S. Zhang, D. V. D. Weide, and J. Oliver, "Superfast phase-shifting method for 3-d shape measurement," *Optics Express*, vol. 18, no. 9, pp. 9684–9689, 2010. [Online]. Available: <http://www.opticsexpress.org/abstract.cfm?URI=oe-18-9-9684>
 - [28] P. Lichtsteiner, C. Posch, and T. Delbruck, "A 128 × 128 120 db 15 μs latency asynchronous temporal contrast vision sensor," *IEEE Journal of Solid-State Circuits*, vol. 43, no. 2, pp. 566–576, 2008.
 - [29] D. M. C. Posch and R. Wohlgenannt, "Aqvg143dbdynamicrange frame-free pwm image sensor with lossless pixel-level video compression and time-domain cds," *IEEE Journal of Solid-State Circuits*, vol. 46, no. 1, pp. 259–275, 2011.
 - [30] J. Leero-Bardallo, T. Serrano-Gotarredona, and B. Linares-Barranco, "A 3.6 s latency asynchronous frame-free event-driven dynamic-vision-sensor," *IEEE Journal of Solid-State Circuits*, vol. 46, no. 6, pp. 1443–1455, 2011.
 - [31] A. G. Andreou and K. A. Boahen, "A contrast sensitive silicon retina with reciprocal synapses," in *Advances in Neural Information Processing Systems*, vol. 4, 1991, pp. 764–772. [Online]. Available: <http://www.stanford.edu/group/brainsinsilicon/pdf/92confNIPSCContrast.pdf>
 - [32] A. Stocker and R. Douglas, "Analog integrated 2-d optical flow sensor with programmable pixels," in *Proceedings of the 2004 International Symposium on Circuits and Systems*, IEEE, Ed., vol. 3, 2004, pp. 9–12.
 - [33] K. Boahen, "Point-to-point connectivity between neuromorphic chips using address events," *IEEE Transactions on Circuits and Systems II: Analog and Digital Signal Processing*, vol. 47, no. 5, pp. 416–434, May 2000.